

## Article

# Simulation of Fuel Consumption Based on Engine Load Level of a 95 kW Partial Power-Shift Transmission Tractor

Md. Abu Ayub Siddique <sup>1</sup>, Seung-Min Baek <sup>2</sup>, Seung-Yun Baek <sup>2</sup>, Wan-Soo Kim <sup>1</sup>, Yeon-Soo Kim <sup>1,3</sup>, Yong-Joo Kim <sup>1,2,\*</sup>, Dae-Hyun Lee <sup>1,\*</sup>, Kwan-Ho Lee <sup>4</sup> and Joon-Yeal Hwang <sup>5</sup>

<sup>1</sup> Department of Biosystems Machinery Engineering, Chungnam National University, Daejeon 34134, Korea; ayub@cnu.ac.kr (M.A.A.S.); ws6602@cnu.ac.kr (W.-S.K.); kimtech612@kitech.re.kr (Y.-S.K.)

<sup>2</sup> Department of Smart Agricultural Systems, Chungnam National University, Daejeon 34134, Korea; bsm1104@o.cnu.ac.kr (S.-M.B.); kelpie0037@o.cnu.ac.kr (S.-Y.B.)

<sup>3</sup> Smart Agricultural Machinery R&D Group, Korea Institute of Industrial Technology (KITECH), Gimje 54325, Korea

<sup>4</sup> CAE Solution Team, TYM ICT Inc., Gongju 32530, Korea; lkh@tymict.com

<sup>5</sup> Smart Solution Team, TYM ICT Inc., Gongju 32530, Korea; fing0828@tymict.com

\* Correspondence: babina@cnu.ac.kr (Y.-J.K.); leedh7@cnu.ac.kr (D.-H.L.); Tel.: +82-42-821-6716 (Y.-J.K.)

**Abstract:** This study is focused on the estimation of fuel consumption of the power-shift transmission (PST) tractor based on PTO (power take-off) dynamometer test. The simulation model of PST tractor was developed using the configurations and powertrain of the real PST tractor. The PTO dynamometer was installed to measure the engine load and fuel consumption at various engine load levels (40, 50, 60, 70, 80, and 90%), and verify the simulation model. The axle load was also predicted using tractor's specifications as an input parameter of the simulation model. The simulation and measured results were analyzed and compared statistically. It was observed that the engine load, as well as fuel consumption, were directly proportional to the engine load levels. However, it was statistically proved that there was no significant difference between the simulation and measured engine torque and fuel consumption at each load level. The regression equations show that there was an exponential relationship between the fuel consumption and engine load levels. However, the specific fuel consumptions (SFC) for both simulation and measured were linear relationships and had no significant difference between them at each engine load level. The results were statistically proved that the simulation and measured SFCs were similar trends. The plow tillage operation could be performed at the gear stage of 7.65 km/h with higher working efficiency at low fuel consumption. The drawback of this study is to use a constant axle load instead of dynamic load. This study can provide useful information for both researchers and manufacturers related to the automated transmission of an agricultural tractor, especially PST tractor for digital farming solutions. Finally, it could contribute to the manufacturers developing a new agricultural tractor with higher fuel efficiency.

**Keywords:** tractor; powershift transmission; fuel consumption; load level; simulation model



**Citation:** Siddique, M.A.A.; Baek, S.-M.; Baek, S.-Y.; Kim, W.-S.; Kim, Y.-S.; Kim, Y.-J.; Lee, D.-H.; Lee, K.-H.; Hwang, J.-Y. Simulation of Fuel Consumption Based on Engine Load Level of a 95 kW Partial Power-Shift Transmission Tractor. *Agriculture* **2021**, *11*, 276. <https://doi.org/10.3390/agriculture11030276>

Academic Editors: Gniewko Niedbala and Sebastian Kujawa

Received: 26 February 2021

Accepted: 20 March 2021

Published: 23 March 2021

**Publisher's Note:** MDPI stays neutral with regard to jurisdictional claims in published maps and institutional affiliations.



**Copyright:** © 2021 by the authors. Licensee MDPI, Basel, Switzerland. This article is an open access article distributed under the terms and conditions of the Creative Commons Attribution (CC BY) license (<https://creativecommons.org/licenses/by/4.0/>).

## 1. Introduction

Tractors, which are machines, deal with various works including agricultural, construction, and forestry [1]. Specifically, agricultural tractors perform various agricultural works such as plow tillage [2], subsurface drainage operation [3], rotary [4], and baler [5]. According to the Mordor Intelligence statistics [6], the global market of agricultural tractors is expected to have 4.02% of annual growth rate in 2025 than that in 2020. Among them, approximately 50% of the tractor global market is in the Asia–Pacific region. In Korea, farmers aged over 65 years old account for 6.7% of the total in 2010; this is expected to be 11.3% in 2050 [7,8]. To compete with the largest tractor manufacturing companies in the global market, and to fulfill the consumers' demands, advanced technologies along with the highest facilities should be introduced.

Advanced technologies such as autonomous, artificial intelligence are applied for agricultural tractors considering driving comfort for aged farmers, higher working efficiency due to lack of labor, and precision farming for increasing production [9]. To confirm the users' flexibility, precise work, and higher efficiencies during operations, several researchers and manufacturers are developing numerous powertrain systems, these include manual transmission (MT), automatic transmission (AT), dual-clutch transmission (DCT), continuously variable transmission (CVT), and power-shift transmission (PST) for agricultural tractors [10,11].

The PST is one of the standard modern tractor systems that is comparatively easier and convenient for the user to control and maintain the vehicle on-field [12]. The PST has two types: the partial PST, which can shift two or more speeds without clutch, having clutch to shift gears, and cannot control machine itself; and the full PST, which can shift all gears without clutching, and the machine can control itself. The PST allows changing gear stages precisely on the run under load conditions of the vehicles [13]. The PST is equipped with a wide range of gear stages without a loss (or minimum) of power during power delivery from engine to driving axles [9]. The PST can apply from low power vehicles to high power vehicles and has become popular as a precise technology. The performance of agricultural machinery varies from nation to nation based on the working environment. Therefore, it is important to conduct the efficiency of the PST tractor.

The fuel consumption of the tractor depends on workloads because the working loads are varied by operation conditions such as engine speed, soil properties of the field, operation types based on implements, and transmission gear stages. Among them, the engine speed and transmission gear stages mostly affect the fuel efficiency of the tractor [14]. The fuel efficiency of the tractor can be optimized by adjusting engine load conditions. The engine load varies on throttle opening of the engine [15]. Therefore, the engine load level of an engine was considered as mostly affected factor to estimate fuel consumption in this study.

Numerous approaches have been proposed to optimize engine speed for improving the fuel efficiency of the tractors. A passive eco-driving system derived for optimal engine speed considering workloads [16]. Jiang [17] developed a PID (proportional-integral-derivative) controller to maintain engine speed for estimating fuel consumption. The performance was reported as better than the existing mechanical governor. Lee [14] developed a model-based controller for fuel consumption based on working loads during plow tillage operation. Therefore, the engine load level is an important factor to estimate the optimal fuel consumption of the agricultural tractors.

The above literature revealed that fuel consumption can be optimized by controlling engine load levels. However, the development of theoretical or model-based control algorithms to control the engine speed is comparatively difficult for highly sensible various tuning methods and has limitations due to time delay, and feedback control process [18]. Moreover, the model-based controllers are needed to validate by field experiment, which requires a tractor installed measurement system that is highly time-consuming and expensive. The only simulation can be an alternative method to minimize cost and experimental time. Saunders [19] developed the discrete element method (DEM) simulation to improve and verify the moldboard plow performance. They believed the simulation method is much more convenient, easier, high accuracy, as well as time-saving. Therefore, a comprehensive, easier, and highly adaptable and reliable simulation method is applied to estimate the fuel consumption in this study.

In addition, digital farming has recently been one of the interesting and value-added topics in automation or unmanned agricultural machinery as well as precision agriculture. As the engine load greatly affects fuel consumption, power transmission efficiency, the decision-making support system of an automatic transmission system or unmanned agricultural vehicles, is one of the key issues for smart digital farming. To address the current issue for digital farming, PTO (power-take-off) dynamometer, which is an indoor test bench, is commercially used as a simple engine load control device in this study. PTO

dynamometer, which does not require a long period to install, and comparatively low cost than that of measurement tractor for measuring the fuel consumption according to the engine load conditions. The engine load is adjusted, controlled, and optimized by the PTO dynamometer load.

This study is a basic study to develop an efficient PST tractor based on different field conditions, implement type, and crop types according to the required hydraulic power, as the PST tractor transmission is performed by the hydraulic pressures. The novelty of this study is that the fuel consumption of the PST tractor was estimated by the simulation method and verified for optimal engine load conditions based on the measured PTO load by PTO dynamometer. Therefore, the objective of this study is to estimate the fuel consumption of PST tractor based on engine load levels using the measured PTO loads by PTO dynamometer. The specific objectives are as follows: (i) to measure engine loads by PTO dynamometer for verifying the simulation model, and (ii) to estimate and analyze the specific fuel consumption of PST tractor.

## 2. Materials and Methods

### 2.1. Tractor Transmission Configurations

In this study, a 95 kW PST tractor (TS130, TYM Co., Ltd., Gongju, Korea) was used to estimate the fuel consumption. The dimension of the tractor (Length  $\times$  Width  $\times$  Height) were 4490  $\times$  2360  $\times$  2940 mm. The rated engine torque is 415 Nm at the rated rotational speed of 2200 rpm. The transmission is power-shift with a combination of 18  $\times$  18 gear stages for both forward and reverse directions. The weight distribution of the PST tractor is 40.3 and 59.7% of the front and rear axle, respectively, whereas the gross weight is 44,587 N. The specifications of the PST tractor were listed in Table 1.

**Table 1.** The specifications of the power-shift transmission (PST) tractor used in this study.

Parameters	Specifications	
Model	TS130, TYM, Korea	
Weight (N)	Gross weight (N)	44,587
	Weight distribution (%)	40.3 and 59.7
Engine	Type	Tier 4
	Rated power (kW)	95
	Rated torque (Nm)	415
	Rated speed (rpm)	2200
	Shifting method	Power-shift
Transmission	Gear stages	6 (1, 2, 3, 4, 5, 6)
	Sub-shifting stages	3 (L, M, H)
	Combinations (forward $\times$ reverse)	18 $\times$ 18
Tire	Model (front and rear)	380/85R24 and 460/85R38
	Diameter (front and rear) (mm)	1256 and 1770

The powertrain of the PST tractor is composed of 2 power shifts (high and low), main clutch: 6 driving shifts (1, 2, 3, 4, 5, and 6) of hydraulic power-shift type and sub-shifting: 3 range shifts (L, M, and H) of mechanical type. The engine power is transmitted to the main clutch dealing with the forward-reverse and high-low shifts. Sequentially the driving shaft is connected to driving shift gear, range shaft gear, and PTO shift gear to drive the rear PTO. This is the partial PST because the sub-shift (Range shift) is performed by a mechanical gear system. The schematic diagram of the powertrain of the partial PST tractor is shown in Figure 1.

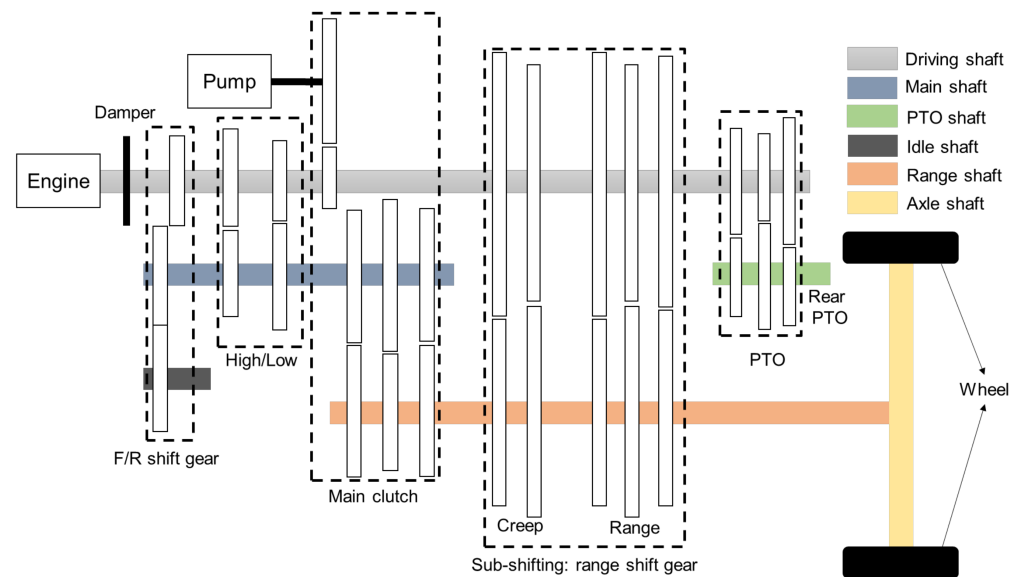


**Figure 1.** The schematic diagram of the PST tractor transmission.

## 2.2. Tractor Dynamic Model

### 2.2.1. Axle Load Prediction

To estimate the fuel consumption of an agricultural tractor, load conditions should be considered. As the main clutch of PST is performed by the hydraulic power, the axle torque cannot predict using the gear ratio of the transmission. Therefore, the axle torque was predicted using tractor specifications. Tractor based prediction model is defined as the theoretical axle torque. Theoretical axle torque of a tractor is calculated under ideal conditions using weight and engine specifications [20]. Both front and rear axle torques of the PST tractor can be calculated using Equations (1)–(4) based on the gross weight of tractor, weight distribution ratio, traction coefficient, and wheel radius.

$$T_f = W_f \times \mu \times r_f, \quad (1)$$

$$T_r = W_r \times \mu \times r_r, \quad (2)$$

$$W_f = W \times \omega_f, \quad (3)$$

$$W_r = W \times \omega_r, \quad (4)$$

where  $T_f$  and  $T_r$  are the front and rear axles torque (Nm), respectively;  $W$ ,  $W_f$ , and  $W_r$  are the gross, front, and rear axle weight of the tractor (N), respectively;  $r_f$  and  $r_r$  are the front and rear wheel tires radius (m), respectively;  $\mu$  is the coefficient of traction (0.8) [21],  $\omega_f$ , and  $\omega_r$  are the weight distribution ratio of both front and rear axles (%), respectively.

### 2.2.2. Specific Fuel Consumption (SFC)

To analyze the actual fuel consumption, the engine loads, which were measured by PTO dynamometer were used to calculate the specific fuel consumption (SFC) [22]. The engine performance of an agricultural tractor is highly affected by fuel efficiency due to the working load variation. It does not mean that fuel consumption is the only factor of fuel efficiency. The SFC is the index of the fuel efficiency that is the work done by an engine per unit horsepower and per unit time. The SFC of an agricultural tractor was calculated using the following Equations (5) and (6) [23].

$$SFC = \frac{FC}{P_{\text{engine}}}, \quad (5)$$

$$P_{\text{engine}} = \frac{2\pi \times T_{\text{engine}} \times N_{\text{engine}}}{60,000}, \quad (6)$$

where FC is the fuel consumption (kg/h); SFC is the specific fuel consumption (g/kWh);  $P_{\text{engine}}$  is the engine power (kW);  $T_{\text{engine}}$  is the engine torque (Nm), and  $N_{\text{engine}}$  is the engine speed (rpm).

### 2.3. Simulation Model of PST Tractor

In this study, the simulation model of PST was developed based on the powertrain of the PST tractor. The simulation model of the PST was developed using the commercial simulation software namely LMS AMESim (version 16, SIEMENS AG, Munich, Germany), which is operated by the 95 kW engine. The engine power is generally divided into the main transmission and rear PTO. The engine power of the main transmission is supplied to the driving axle through the high-low, hydraulic clutch pack (main clutch), and mechanical sub-shifting (range shifts: creep and range). In the PST, the constructions of three main clutch packs are the same. Therefore, the simulation model was simplified and conducted simulation using one main clutch pack to estimate the fuel consumption precisely. In this study, the measured data and engine characteristics map were applied to conduct and verify the simulation model of the PST. The predicted axle load was also used as an input parameter to characterize the simulation model as a real PST tractor used in this study. The simulation model of the entire PST tractor was shown in Figure 2.

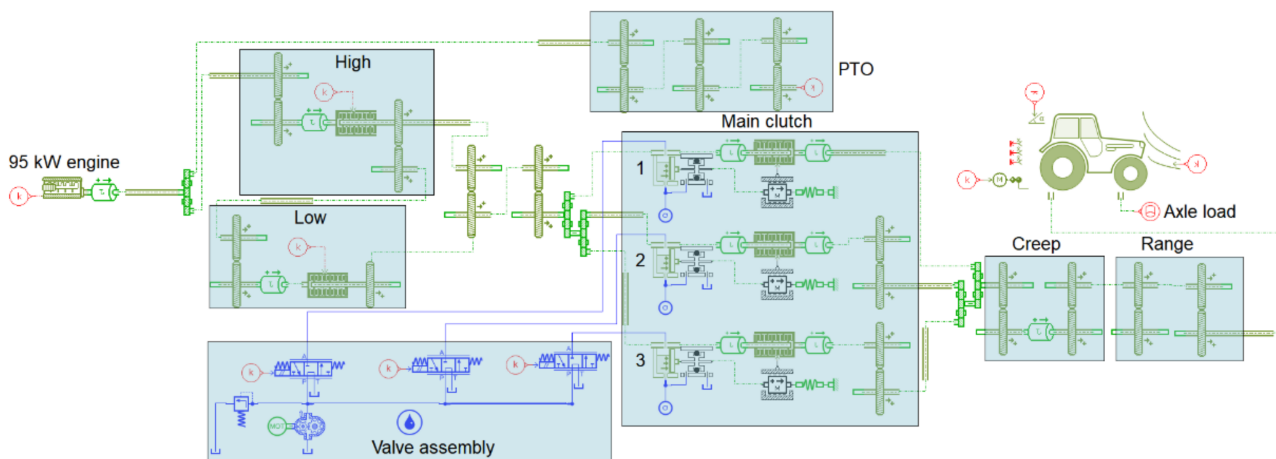


**Figure 2.** The simulation model of the entire PST tractor used in this study.

### 2.4. Dynamometer Test Bench and Specifications

In this study, a PTO dynamometer, which is an indoor test bench was installed to measure the fuel consumption of the PST tractor according to the engine speed. The fuel consumption measurement device (REO-CFMT, 3R Co., Ltd., Siheung, Korea), is used in this study. The PTO dynamometer was connected to the rear PTO of the PST tractor and the engine load was adjusted by controlling the dynamometer load. Quantum X (HBM: MX840B) data acquisition system (DAQ) was used to measure the dynamometer load and fuel consumption of the PST tractor. Using the measured fuel consumption, the SFC of the PST tractor was determined at various throttle levels of engine. The experiment of the PTO dynamometer test was carried out by [24]. The PTO dynamometer test bench was shown in Figure 3.

In this study, the engine load levels were divided into six levels like 40, 50, 60, 70, 80, and 90%. The full load (100%) condition was applied to develop the engine characteristics map to conduct the simulation because the fuel consumption of tractor can be optimized by operating the engine at full load condition [25,26]. Farias et al. [27] also considered not less than 30% of the engine load level. According to the Nebraska tractor test, the SFC increases

for more than 30% of engine loads [28]. Because the engine is required to have very low speed and longer gears; also, the tractor is required to apply withstanding its load.

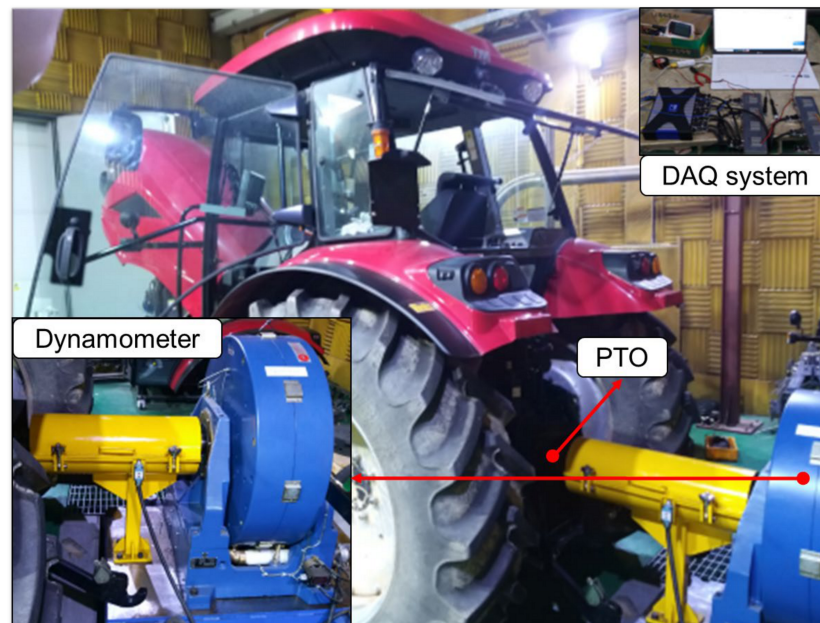


**Figure 3.** The PTO dynamometer test bench used in this study.

The eddy current type PTO dynamometer (SE 500, SAJ, Pune, India) was used in this study. This type of dynamometer offers a wide range of capacities from 5 to 720 kW for engine test. In this study, a 500 kW PTO dynamometer was installed and the load cell type was U4000. It has the precision strain gauge load cell torque measurement system that provides high accuracy torque measurement for engine test, where was maximum torque of 3000 Nm at 1800 rpm. The accuracy of this dynamometer:  $\pm 0.25\%$  of the rated torque and  $\pm 1\%$  of speed, where was the speed range of 1600~4500 rpm. The detailed specifications of the PTO dynamometer used in this study were listed in Table 2.

**Table 2.** The specifications of the dynamometer used in this study.

Parameters	Specifications
Model	SE 500, SAJ, India
Type	EDDY Current
Maximum power (kW)	500
Maximum torque (Nm)	3000 @1800 rpm
Speed (rpm)	1600~4500
Inertia (kgm <sup>2</sup> )	2.196
Load cell type	U4000
Weight (kg)	1500

## 2.5. Simulation Procedures

### 2.5.1. Model Verification and Generalization

The raw data, which were measured using PTO dynamometer were preprocessed by data filtering. The data filtering was used to remove the observations that contain the errors or undesirable observations for analysis and applied in the simulation model for verifying the model. The entire measured data were 12 sets, which were divided into 7 and 5 sets for the calibration and validation, respectively, in this study. The calibration datasets were applied to the simulation model of the PST tractor to determine the hourly fuel consumption and finally, the specific fuel consumptions were calculated. The validation datasets were used to verify the simulation model.

In this study, the plow tillage load was also applied to generalize the verified simulation model. The representative plow tillage load data was calculated from literature [14]. To select the suitable gear stage at low fuel consumption, the representative load data was plotted in the engine performance curve that generalized the simulation model for agricultural operations. Because, the engine performance curve has two regions: one is governed region which was controlled by governor, and another is the ungoverned region which was controlled by the engine load. Generally, the fuel consumption is comparatively low before ungoverned region but the engine might be shut down at a low speed due to the working load fluctuations. Moreover, the fuel consumption in the governed region was higher whereas was the engine torque is lower. Tractor might be unable to perform field operations at high load conditions. Therefore, the plow load data should be plotted on the engine performance curve to select a suitable gear stage for plow operation. The procedure of the model verification and generalization is shown in Figure 4.

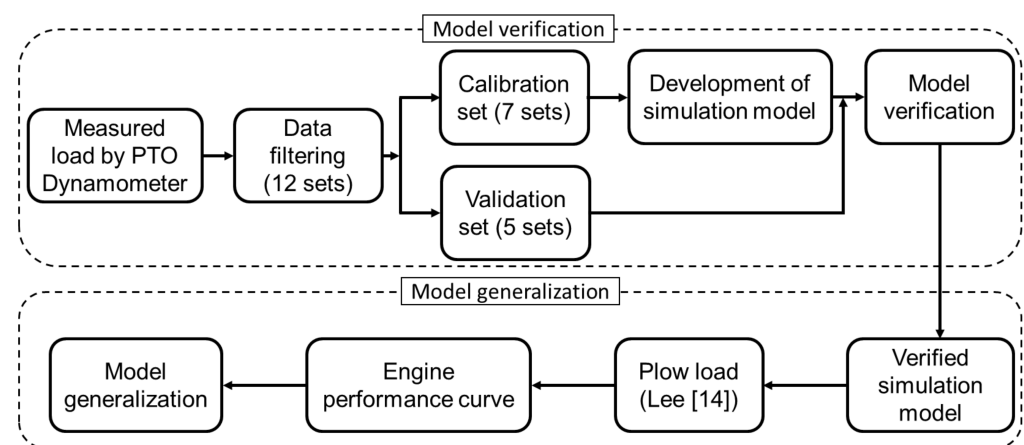


**Figure 4.** The block diagram of model verification and generalization used in this study.

### 2.5.2. Engine Characteristics Map

The engine static torque is a function of engine speed and throttle level [10,29]. The mathematical model of engine torque is in Equation (7) for a 95 kW engine.

$$T_{\text{engine}} = f(N_{\text{engine}}, a), \quad (7)$$

where  $T_{\text{engine}}$  is the engine torque (Nm);  $N_{\text{engine}}$  is the engine speed (rpm), and  $a$  is the throttle level (%).

Throttle level means to control the engine power by regulating the fuel amount to enter into the engine. Engine throttle opening greatly depends on throttle angles [30]. In this study, the engine characteristics map was developed using AMESim 3D graphical platform. The engine characteristic map was developed for engine full load (100%) condition from engine test. The engine torque was calculated at each throttle level (%) using Equation (7), which was applied to develop the static engine map used in this study, whereas the maximum torque was 500 Nm at 1600 rpm for 100% of throttle opening. The simulation was conducted using the developed engine map, shown in Figure 5.

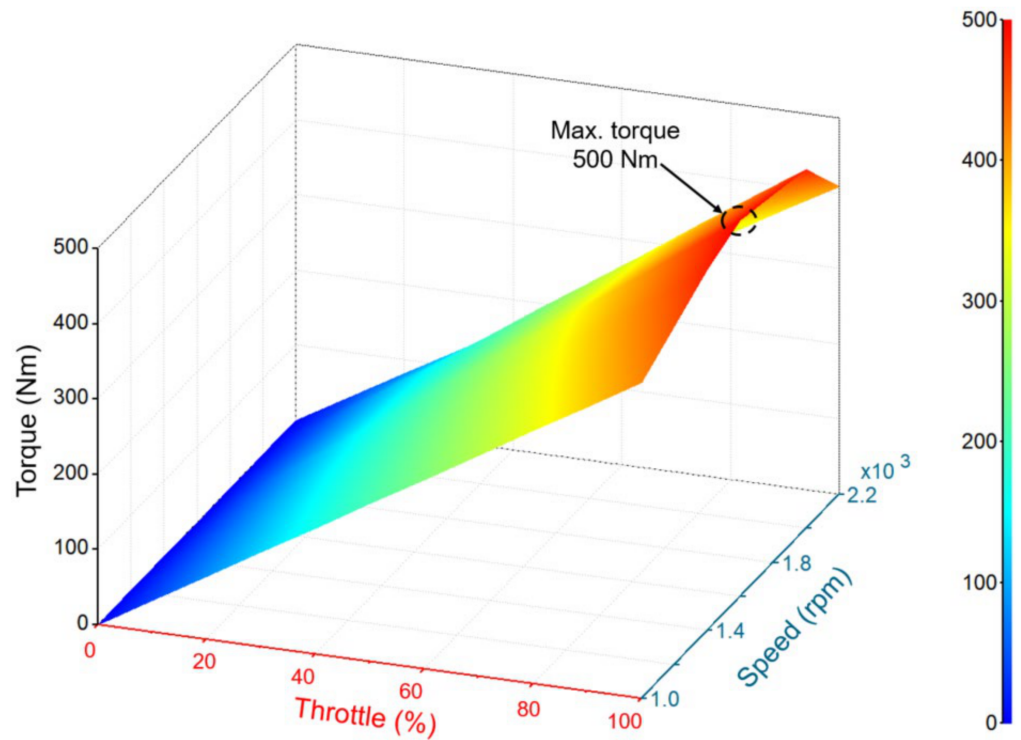


Figure 5. The 95 kW engine map used in this study.

2.5.3. Simulation Parameters

The block diagram of the simulation procedure was shown in Figure 6. The engine power is divided into the transmission and rear PTO of the tractor. The transmission power supplied by the forward-reversed shaft was delivered to the driving axle through the high-low, the main clutch operated hydraulically, and mechanical sub-shifting. In this study, the measured load was applied in the rear PTO to conduct the simulation. The axle load was also predicted using a theoretical model, where the specifications of a real PST tractor were used, and a 95 kW engine was applied in the simulation model. The engine characteristics map (Figure 5) was applied to the engine.

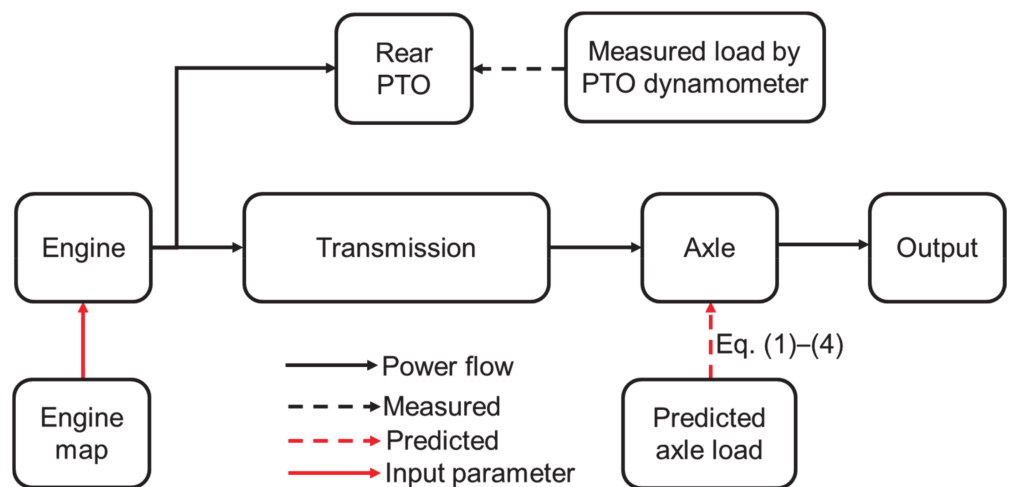


Figure 6. The block diagram for applied simulation parameters in this study.

2.6. Analysis Method

In this study, several statistical approaches were used in this study to evaluate the estimated fuel consumptions for both simulation and measured experiment. One-way

ANOVA (Analysis of variance), and Duncan's multiple range test (DMRT) were performed to analyze the significance of the engine torque for both simulation and experimental methods with respect to the throttle level of the engine. The fuel consumption was also analyzed statistically. The software used for the analysis was IBM SPSS Statistics (SPSS 25, SPSS Inc., New York, NY, USA). The error and accuracy of the SFC for various throttle levels were analyzed for both simulation and experimental methods by regression methods. The coefficient of determination and p-value were also determined. The R-square value, which is over 0.90 is considered reliable for comparison between two variables [31]. The R-squared can be obtained by the following Equation (8).

$$R^2 = 1 - \frac{\sum_i (y_i - \hat{y}_i)^2}{\sum_i (y_i - \bar{y})^2}, \quad (8)$$

where  $R^2$  is the regression coefficients of the SFC for both methods;  $y_i$  is the  $i$ th measured SFC (g/kWh);  $\hat{y}_i$  is the  $i$ th simulation SFC (g/kWh), and  $\bar{y}$  is the mean of the measured SFC (g/kWh).

The simulation and experimental methods by PTO dynamometer test to measure the SFC of the tractor were also compared statistically and determined the accuracy and error by the root mean square error (RMSE) and relative deviation (RD) along with the R-squared value for both methods. The RMSE and RD can be obtained using the following Equations (9) and (10).

$$\text{RMSE} = \sqrt{\frac{1}{N} \sum_i (\hat{y}_i - y_i)^2}, \quad (9)$$

$$\text{RD} = \frac{\text{RMSE}}{\text{Mean}} \times 100, \quad (10)$$

where  $N$  is the number of the total SFC data; RMSE is the root mean square error of the SFC (%), and RD is the relative deviation of the SFC (%), which was calculated by the ratio of the RMSE to the mean of the SFC of the tractor.

### 3. Results

#### 3.1. Engine Torque

In this study, engine torque was measured based on the engine load levels (40, 50, 60, 70, 80, and 90%) by installing PTO dynamometer and the simulation model was calibrated to conduct the simulation of the model. It was observed that the engine torques were gradually increased and reached the maximum engine torques for each load level at 1600 rpm of the engine speed. After then, the engine torques decreased gradually until the engine speed of 2200 rpm. It was noticed that there was a similar trend for both simulation and measured engine torques. Even there was almost the same increasing rate of the engine torque for each load level.

It was observed that the highest maximum engine torques for both simulation and measured were found at 90% of load level and the lowest maximum torques for both methods were at 40% of load level. It means that the engine torques were increasing with an increasing rate of the engine load levels. The results indicate that the engine torques were directly proportional to the engine load levels. Both simulation and measured engine torques were shown in Figure 7.

After analyzing, it was found that the highest maximum engine torques for both simulation and measured were 455 and 450 Nm at 90% of load level, respectively. The lowest maximum torques for both methods were also found 200 Nm at 40% of load level. The simulation and measured engine torques were also compared statistically using ANOVA along with DMRT test. It was noticed that there was no significant difference among the simulation and measured engine torques at each load level, where the p-value was less than the significant value of 5%. The ANOVA along with DMRT test results of both simulation and measured engine torques were listed in Table 3.

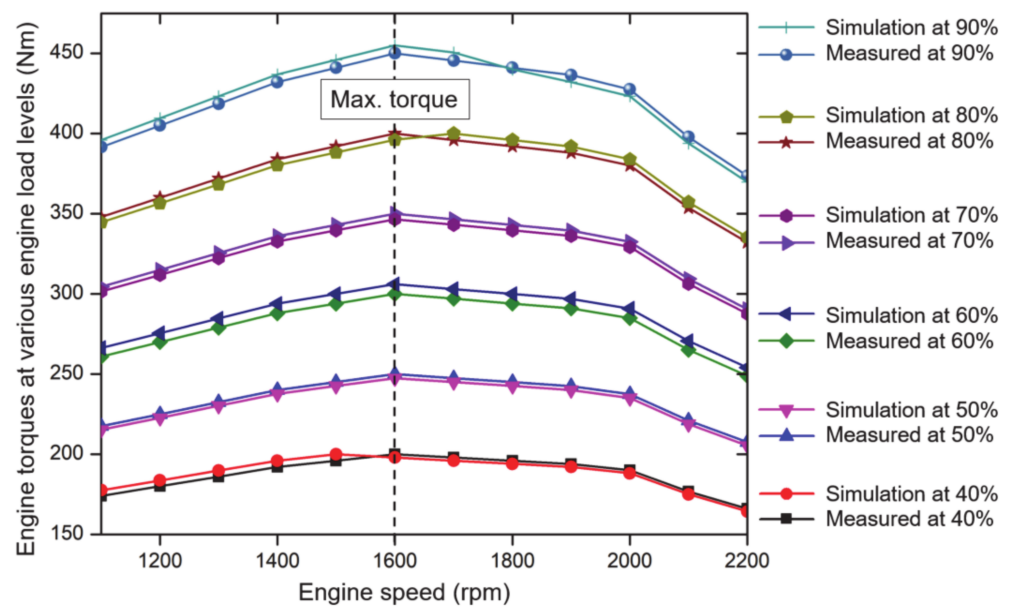


Figure 7. The measured and simulation engine torques at various load levels.

Table 3. The statistical analysis of both simulation and measured engine torques at various engine load levels.

Method	Simulation Engine Torques (Nm)						p-Value
Load Levels (%)	40	50	60	70	80	90	
Maximum	200	247.52	306.12	346.53	400	455	0.000
Minimum	164.36	205.45	254.08	287.62	335	369.80	
Avg. ± S.D.*	186.62 ± 11.30 <sup>a</sup>	230.08 ± 14.49 <sup>b</sup>	284.55 ± 17.92 <sup>c</sup>	322.11 ± 20.28 <sup>d</sup>	371.76 ± 23.70 <sup>e</sup>	419.41 ± 28.07 <sup>f</sup>	
Method	Measured Engine Torques (Nm)						
Maximum	200	250	300	350	400	450	
Minimum	166	207.50	249	290.50	332	373.50	
Avg. ± S.D.*	185.91 ± 11.71 <sup>a</sup>	232.38 ± 14.63 <sup>b</sup>	278.86 ± 17.56 <sup>c</sup>	325.34 ± 20.48 <sup>d</sup>	371.81 ± 23.41 <sup>e</sup>	418.29 ± 26.34 <sup>f</sup>	

<sup>a,b,c,d,e,f</sup> Means within each column with the same lettering are not significantly different at  $p < 0.05$  according to Duncan’s multiple range test. \* Avg. ± S.D. is the Average ± Standard Deviation.

### 3.2. Specific Fuel Consumption (SFC)

In this study, the fuel consumption was measured to estimate the SFC. Figure 8 shows the simulation and measured hourly fuel consumption at six levels (40, 50, 60, 70, 80, and 90) of engine load. It was observed that fuel consumption of both simulation and measured were also increasing sharply with an increase of the engine load levels. For load levels of 40, 50, and 60%, the increasing rate of fuel consumption was almost parallel with each other. In the case of 70% of engine load level, the fuel consumption was dramatically increased after 2000 rpm of engine speed. For 80 and 90% of engine load levels, the fuel consumptions were also parallel between them but there were comparatively higher mean differences from the fuel consumption of 70% of engine load level.

The highest and lowest maximum hourly fuel consumptions for both simulation and measured were found around 20.22 and 19.95, and 6.42 and 6.55 kg/h at 90 and 40% of engine loads, respectively. It was observed that the average increasing rate for both simulation and measured fuel consumption were comparatively higher at 70% of engine load than that of other load levels, accounting for 8.45 and 8.60 kg/h, whereas the average fuel consumptions for both simulation and measured at 60 and 80% of engine loads were 6.14 and 6.24, and 12.93 and 11.56 kg/h, respectively. The statistical analysis results show that there was no significant difference between simulation and measured hourly fuel consumption at each load level because the statistical analysis proved that the p-value between the simulation and measured fuel consumption was less than the significance level of 5%. The statistical analysis results of hourly fuel consumptions for both methods were listed in Table 4.

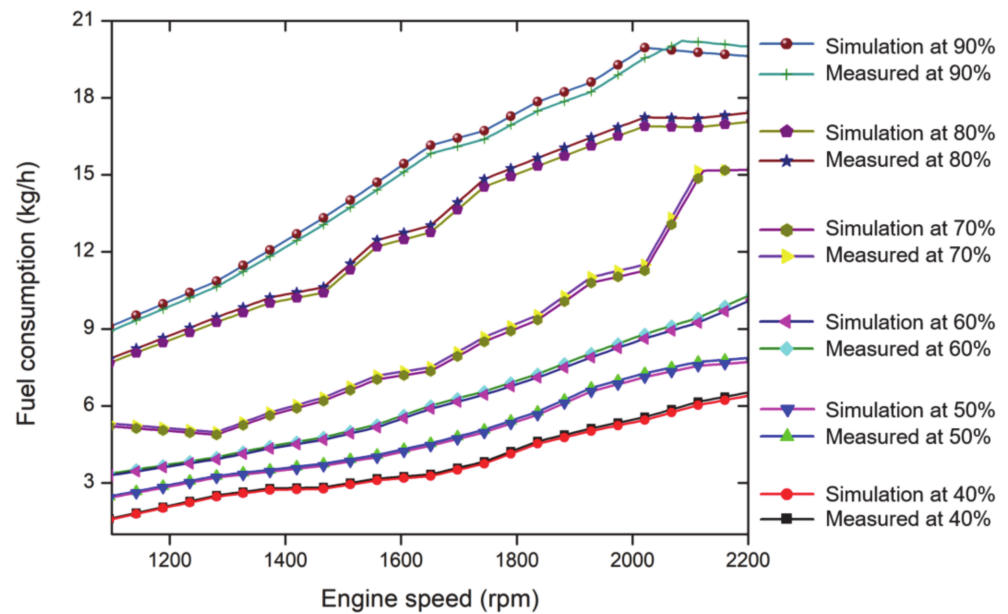


Figure 8. The simulation and measured hourly fuel consumption at various load levels.

Table 4. The statistical analysis of both simulation and measured hourly fuel consumptions at various engine load levels.

Method	Simulation Fuel Consumption (kg/h)						p-Value
Load Levels (%)	40	50	60	70	80	90	
Max. at 2200 rpm	6.42	7.72	10.14	15.19	17.08	20.22	0.000
Min. at 1100 rpm	1.57	2.42	2.42	4.88	7.67	8.90	
Avg. ± S.D.	3.76 ± 1.41 <sup>a</sup>	4.88 ± 1.70 <sup>b</sup>	6.14 ± 2.04 <sup>c</sup>	8.45 ± 3.23 <sup>d</sup>	12.93 ± 3.18 <sup>e</sup>	15.15 ± 3.65 <sup>f</sup>	
Method	Measured Fuel Consumption (kg/h)						0.000
Max. at 2200 rpm	6.55	7.88	10.35	15.19	17.43	19.95	
Min. at 1100 rpm	1.61	2.47	3.36	4.98	7.83	9.08	
Avg. ± S.D.*	3.84 ± 1.44 <sup>a</sup>	4.98 ± 1.73 <sup>b</sup>	6.27 ± 2.09 <sup>c</sup>	8.60 ± 3.23 <sup>d</sup>	11.56 ± 3.25 <sup>e</sup>	15.35 ± 3.58 <sup>f</sup>	

<sup>a,b,c,d,e,f</sup> Means within each column with the same lettering are not significant different at  $p < 0.05$  according to Duncan’s multiple range test.

\* Avg. ± S.D. is the Average ± Standard Deviation.

In this study, both simulation and measured hourly fuel consumptions (FC) were used to calculate the SFC of the engine. Further, the engine power ( $P_{engine}$ ) was calculated from the measured engine torque and speed to determine the SFC (g/kWh). Figure 9 shows the average SFC of the engine for both simulation and measured at different load levels. The regression equations (y) of the SFC of both simulation and measured with respect to the engine load levels represented that the SFC of both simulation and measured were increased almost 13.66 and 13.94 g/kWh, respectively for each 10% increase of engine loads. It indicates the engine load levels have a significant effect on the SFC of the PST tractor. From regression equations, it was also observed that the SFC of both methods were an exponential relationship with different engine load levels. The R-squared of both simulation and measured SFC were found almost 0.9831 and 0.9835, respectively.

The ANOVA and DMRT test results of the SFC for both simulation and measured at various load levels were listed in Table 5. The analysis results show that there was no significant difference between the simulation and measured SFC at the significance level of 5%, whereas the standard error (SE) was 1.14. The maximum average (Avg. ± S.D.) SFC of both simulation and measured were  $239.91 \pm 51.37$  and  $244.81 \pm 52.41$  g/kWh, respectively at 90% of engine load level, whereas the minimum average (Avg. ± S.D.) SFCs were calculated at 40% of engine load, accounting for approximately  $51.35 \pm 9.81$  and  $52.40 \pm 10.01$  g/kWh for both simulation and measured methods, respectively.

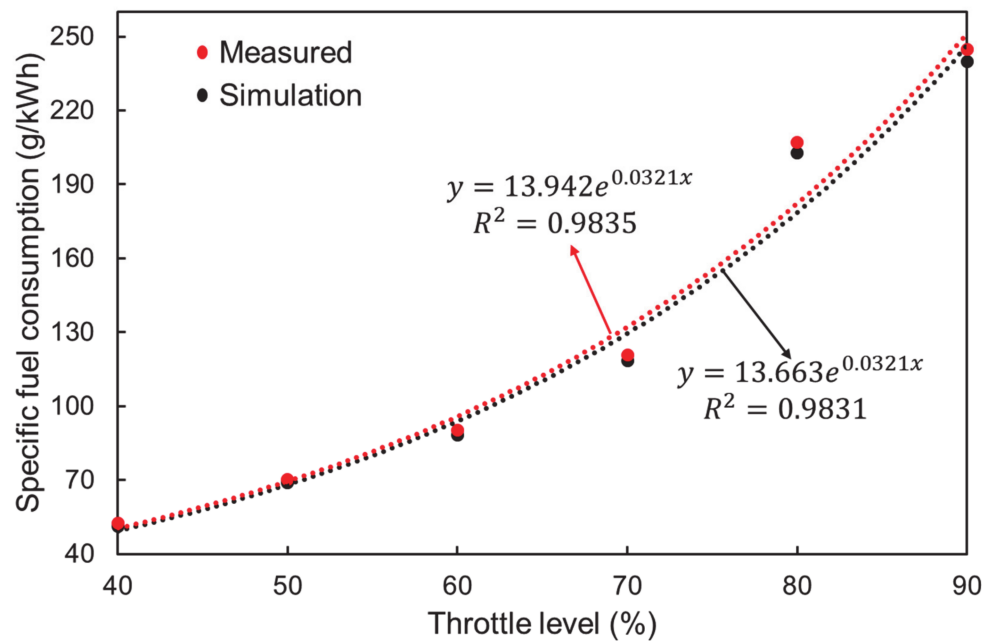


**Figure 9.** The regression of the average measured and simulation Specific Fuel Consumption (SFC) at various load levels.

**Table 5.** The statistical analysis of both simulation and measured specific fuel consumptions (SFC) at various engine load levels.

Method	Specific Fuel Consumption (g/kWh)						p-Value	SE	
	Load Levels (%)	40	50	60	70	80			90
Simulation		51.35 ± 9.81 <sup>a *</sup>	68.81 ± 14.22 <sup>b</sup>	118.71 ± 18.71 <sup>c</sup>	118.46 ± 30.24 <sup>d</sup>	202.92 ± 44.86 <sup>e</sup>	239.91 ± 51.37 <sup>f</sup>	0.000	1.14
Measured		52.40 ± 10.01 <sup>a</sup>	70.21 ± 14.51 <sup>b</sup>	90.14 ± 19.09 <sup>c</sup>	120.88 ± 30.24 <sup>d</sup>	207.06 ± 45.78 <sup>e</sup>	244.81 ± 52.41 <sup>f</sup>		

<sup>a,b,c,d,e,f</sup> Means within each column with the same lettering are not significant different at  $p < 0.05$  according to Duncan’s multiple range test.  
 \* Average ± Standard Deviation.

To identify the similarity, accuracy, tendency, and error between the simulation and measured SFC, linear regression,  $R^2$ , RMSE, and RD were calculated. Figure 10 shows the regression analysis of SFC for both methods. The R-squared value was 0.99, whereas the RMSE and RD were found approximately 1.89% and 2.54%. From the regression equation (y), it is clear that the simulation and measured SFCs were a linear relationship between each other. The results indicate that the SFC for both simulation and measured were a similar trend.

It is important to generalize the simulation model at low fuel consumption and high engine torque for agricultural operations. Therefore, the representative plow tillage load data was plotted in the engine performance curve (Figure 11). It was observed that the SFC was steadily increasing after 1500 rpm of the engine. It means that the engine should operate at a low speed to reduce fuel consumption. However, the working efficiency would be lower at low engine speed. It might suddenly turn off the engine due to the fluctuation of loads. Therefore, the engine speed should be adjusted within the ungoverned region where the working efficiency was comparatively higher but the fuel consumption was relatively lower.

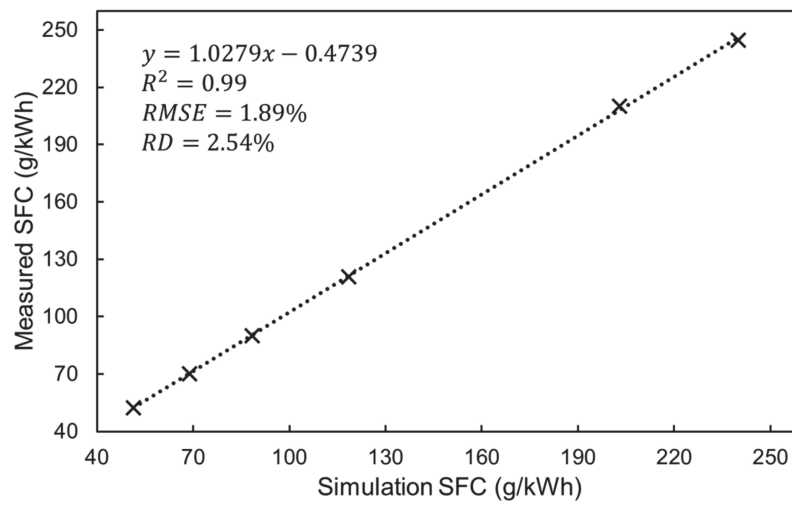


Figure 10. The linear regression of the average simulation and measured SFC.

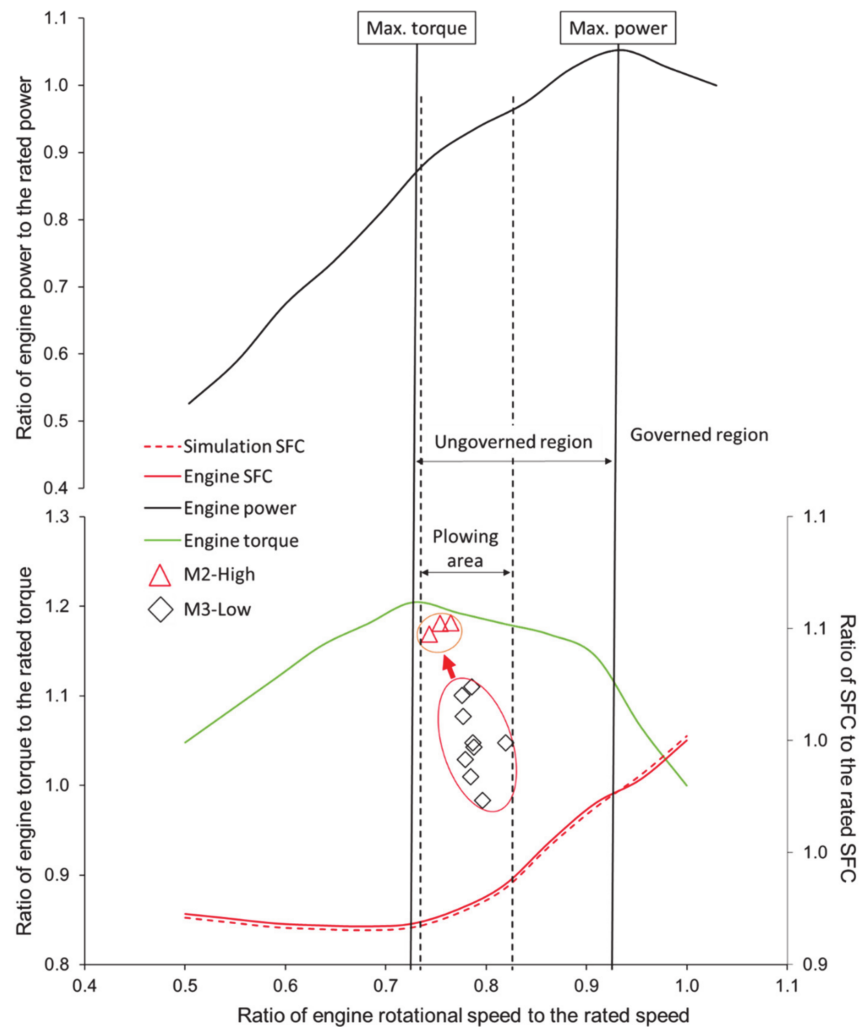


Figure 11. The engine performance curve at engine full load condition.

The plow operation loads, which were calculated comparing with the literature [14], were performed for two gear selections. M2-High and M3-Low were 7.56 km/h and 9.81 km/h, respectively, which were selected to perform plow tillage at the same agricultural field. The ratios of the calculated torque to the rated torque were presented in Figure 11. It

showed that the plow tillage operation loads belonged to the ungoverned region of the engine performance curve, where the plowing at the gear stage of 7.56 km/h was relatively low fuel consumption and high working load for full engine load conditions. In the case of the 9.81 km/h gear stage, the fuel consumption was comparatively higher with low working load.

#### 4. Discussion

In this study, the engine torque and fuel consumption of the PST tractor were measured at various engine load levels (40, 50, 60, 70, 80, and 90%); also, the simulation model of the PST tractor was verified by the measured PTO load data. The results of this study were discussed as below:

- (1) It was noted that the engine torques for both simulation and measured were directly proportional to the engine load level. The statistical analysis (DMRT) proved that there was no significant difference between the simulation and measured engine torque at each load level. Kolator and Bialobrzewski [32] reported that engine load condition has a highly significant effect on tractor performance.
- (2) It was observed that the increasing rates of the fuel consumptions were parallel with each other and sharply increased with respect to the engine speed. Only for 70% of engine load level, the fuel consumption was dramatically increased after 2000 rpm of engine speed. It might be caused by an excessive flow that is the main reason for fuel losses [33]. Those results indicate that the hourly fuel consumptions were also directly proportional to the engine load levels. The SFCs at various engine load levels were analyzed statistically. The statistical analysis showed that there was no significant difference between the simulation and measured SFC as the significant level of 5%. The regression analysis with respect to throttle level showed that the increasing rate for both the simulation and measured SFCs at each load level. The results indicated that the engine load levels have a highly significant effect on the SFC of the PST tractor. Shafaei [31] reported over 0.90 of R-squared value will be reliable to verify the relationship. From the regression equation, it is clear that there was an exponential relationship between the SFC and engine load levels.
- (3) To distinguish the similarity, accuracy, and error between the simulation and experimental methods to estimate the SFC, statistical tests (R-squared, RMSE, and RD) were also conducted. From the regression equation, it was clear that there was a linear relationship between the simulation and measured SFC. The statistical results proved that the simulation SFC was similar to the measured SFC.
- (4) It was observed that the engine generated power was higher at 9.81 km/h (M3-Low) than the soil strength, which indicated the loss of power. It was believed that the power loss had occurred by the travel reduction ratio (slip) [34]. The results indicated that the gear selection of 7.56 km/h (M2-High) was highly beneficial to conduct plow tillage operation using the 95 kW partial PST tractor considering high engine torque. To optimize the fuel consumption, the gear selection should be shifted to the M2-High instead of M3-Low because M3-Low generates low engine torque that might be suddenly turn-off the engine due to high soil strength [14].

In addition, several researchers proved the reliability of the simulation method based on comfortability, easier, and convenience. The simulation method, which has also been reliable to conduct the performance, design, estimation, and evaluation [35] of the agricultural machinery, reduce labor cost and time-consuming instead of field experiment [36]. The results revealed that the PTO dynamometer can easily control the engine load to estimate fuel consumption. As the simulation results of SFC represent the PTO dynamometer measured SFC results, the simulation results can be commercially applied to improve the fuel efficiency of the PST tractor. Finally, this study can contribute to the manufacturers to develop a new agricultural tractor with high fuel efficiency.

## 5. Conclusions

This study was emphasized to simulate the fuel consumption of the PST tractor. The simulation of the PST tractor was developed using the configurations and powertrain of the real PST tractor manufactured by the Korean company. The PTO dynamometer, an indoor test bench, was installed to measure the engine load and fuel consumption at various throttle levels (40, 50, 60, 70, 80, and 90%) of the PST tractor according to the engine speed. The tractor axle load was predicted using the specifications of the tractor as an input parameter of the simulation model. The major findings of this study were listed as below:

- (1) It was observed that the highest maximum engine torques for both simulation and measured were 455 and 450 Nm at 90% of engine load, respectively. The lowest maximum torques for both methods were also found at 200 Nm at 40% of engine load. It was also observed that the maximum engine torques for both simulation and measured were at 1600 rpm of engine speed for all engine throttle levels. The statistical analysis (DMRT) proved that there was no significant difference between the simulation and measured engine torque at each throttle level. However, it was noticed that the engine torques for both simulation and measured were directly proportional to the engine throttle level.
- (2) The highest and lowest maximum hourly fuel consumptions for both simulation and measured were found around 20.22 and 19.95, and 6.42 and 6.55 kg/h at 90 and 40% of engine load, respectively. It was observed that the average increasing rate for both simulation and measured fuel consumption were comparatively higher at 70% of engine load than that of other engine load levels, accounting for 8.45 and 8.60 kg/h. The regression equations of the SFC of both simulation and measured with respect to the engine throttle levels represented that the SFC of both simulation and measured were increased almost 13.66 and 13.94 g/kWh, respectively for each 10% increase of engine load. The R-squared of both simulation and measured SFC were found almost 0.9831 and 0.9835, respectively. The analysis results show that there was no significant difference between the simulation and measured SFC, whereas the standard error (SE) was 1.14. The R-squared value was 0.99, whereas the RMSE and RD were approximately 1.89% and 2.54%, respectively.

In summary, the engine torques were directly proportional to the engine load levels. The statistical analysis (DMRT) proved that there was no significant difference between the simulation and measured engine torques. The simulation and measured SFCs were an exponential relationship with various engine load levels. However, both simulation and measured SFCs were linearly relationship and have statistically no significant difference between them. It was also found a similar trend for both methods.

The drawback of this study is the prediction load using tractor and engine specifications, which were applied to the axle, were constant. Howard [37] conducted the fuel efficiency of the continuously variable transmission (CVT) tractor with respect to drawbar power that was a dynamic load [38]. Gui [28] suggested applying the engine speed controller to estimate the optimal fuel efficiency of the agricultural tractor. Lee [14] also developed the engine speed control system to improve fuel efficiency and verify by tillage operation, which was also a dynamic workload. Finally, it can be said that the field operation is needed to estimate the fuel efficiency for commercialization. However, it is planned to conduct field operations considering various types of implements based on major agricultural operations.

In conclusion, it can be said that PTO dynamometer, which can control the engine loads to estimate the fuel consumption, minimize labor cost and time rather than field operations, and this study can be helpful to the manufacturers to develop and improve a new agricultural tractor with higher fuel efficiency. It could be recommended that the users should perform the plow tillage at the gear stage of 7.65 km/h for low fuel consumption with respect to higher working efficiency. This study could also contribute to digital farming by improving fuel efficiency, which was the key issue for the automated transmission of an agricultural tractor. In the future, it is planned to conduct field operations based on

implements type and crops for dynamic load data, and field data will be stored in a server system, which is a core goal of smart digital farming for an agricultural machinery sector.

**Author Contributions:** Conceptualization, M.A.A.S. and Y.-J.K.; methodology, M.A.A.S., W.-S.K., and Y.-J.K.; software, M.A.A.S.; validation, M.A.A.S., Y.-S.K., S.-M.B.; S.-Y.B.; K.-H.L., and J.-Y.H. formal analysis, M.A.A.S.; investigation, W.-S.K., Y.-S.K., S.-M.B., S.-Y.B.; K.-H.L.; J.-Y.H., and Y.-J.K., and D.-H.L.; writing—original draft preparation, M.A.A.S.; writing—review and editing, M.A.A.S., and D.-H.L.; visualization, M.A.A.S., D.-H.L., and Y.-J.K.; supervision, Y.-J.K.; project administration, Y.-J.K.; funding acquisition, Y.-J.K. All authors have read and agreed to the published version of the manuscript.

**Funding:** This work was carried out with the support of “Cooperative Research Program for Agriculture Science and Technology Development (Project No. PJ01498102)” Rural Development Administration, Republic of Korea.

**Institutional Review Board Statement:** Not applicable.

**Informed Consent Statement:** Not applicable.

**Data Availability Statement:** The data presented in this study are available within the article.

**Conflicts of Interest:** The authors declare no conflict of interest.

## References

- Kim, W.S.; Kim, Y.J.; Kim, Y.S.; Baek, S.Y.; Baek, S.M.; Lee, D.H.; Nam, K.C.; Kim, T.B.; Lee, H.J. Development of control system for automated manual transmission of 45-kW agricultural tractor. *Appl. Sci.* **2020**, *10*, 2930. [CrossRef]
- Shafaei, S.M.; Loghavi, M.; Kamgar, S. Fundamental realization of longitudinal slip efficiency of tractor wheels in a tillage practice. *Soil Tillage Res.* **2021**, *205*, 104765. [CrossRef]
- Islam, M.N.; Iqbal, M.Z.; Kabir, M.S.N.; Jung, K.Y.; Mun, D.H.; Chung, S.O. Performance Evaluation of Trenchless Subsurface Drainage Piping Machine. *J. Biosyst. Eng.* **2019**, *44*, 218–225. [CrossRef]
- Mairghany, M.; Yahya, A.; Adam, N.M.; Mat Su, A.S.; Aimrun, W.; Elsoragaby, S. Rotary tillage effects on some selected physical properties of fine textured soil in wetland rice cultivation in Malaysia. *Soil Tillage Res.* **2019**, *194*, 104318. [CrossRef]
- Kim, W.S.; Kim, Y.J.; Baek, S.M.; Moon, S.P.; Lee, N.G.; Kim, Y.S.; Park, S.U.; Choi, Y.; Kim, Y.K.; Choi, I.S.; et al. Fatigue life simulation of tractor spiral bevel gear according to major agricultural operations. *Appl. Sci.* **2020**, *10*, 8898. [CrossRef]
- Mordor Intelligence. Available online: <https://www.mordorintelligence.com/industry-reports/india-agricultural-tractormachinery-%0Amarket> (accessed on 16 March 2021).
- Kim, Y.S.; Lee, P.U.; Kim, W.S.; Kwon, O.W.; Kim, C.W.; Lee, K.H.; Kim, Y.J. Strength analysis of a PTO (Power Take-Off) gear-train of a multi-purpose cultivator during a rotary ditching operation. *Energies* **2019**, *12*, 1100. [CrossRef]
- Siddique, M.A.A.; Kim, W.S.; Kim, Y.S.; Kim, T.J.; Choi, C.H.; Lee, H.J.; Chung, S.O.; Kim, Y.J. Effects of temperatures and viscosity of the hydraulic oils on the proportional valve for a rice transplanter based on PID control algorithm. *Agriculture* **2020**, *10*, 73. [CrossRef]
- Tanelli, M.; Panzani, G.; Savaresi, S.M.; Pirola, C. Transmission control for power-shift agricultural tractors: Design and end-of-line automatic tuning. *Mechatronics* **2011**, *21*, 285–297. [CrossRef]
- Siddique, M.A.A.; Kim, W.S.; Kim, Y.S.; Baek, S.Y.; Baek, S.M.; Kim, Y.J.; Park, S.U.; Choi, C.H. Simulation of Design Factors of a Clutch Pack for Power-Shift Transmission for an Agricultural Tractor. *Sensors* **2020**, *20*, 7293. [CrossRef]
- Liyou, X.; Yihao, Z.; Jinzhong, S.; Xianghai, Y. Optimization of power shift tractor clutch based on ahp and improved genetic algorithm. *Acta Tech.* **2017**, *62*, 373–384.
- Siddique, M.A.A.; Kim, T.J.; Kim, Y.J. Technical Trend of the Power Shift Transmission (PST) of Agricultural Tractor. *J. Drive Control* **2020**, *17*, 68–75.
- Liang, J.; Yang, H.; Wu, J.; Zhang, N.; Walker, P.D. Power-on shifting in dual input clutchless power-shifting transmission for electric vehicles. *Mech. Mach. Theory* **2018**, *121*, 487–501. [CrossRef]
- Lee, J.W.; Kim, S.C.; Oh, J.; Chung, W.J.; Han, H.W.; Kim, J.T.; Park, Y.J. Engine speed control system for improving the fuel efficiency of agricultural tractors for plowing operations. *Appl. Sci.* **2019**, *9*, 3898. [CrossRef]
- Grisso, R.; Pitman, R.; Perumpral, J.V.; Roberson, G.T. Gear up and Throttle down to Save Fuel. In *Virginia Cooperative Extension*; Virginia Tech.: Blacksburg, VA, USA, 2010; pp. 442–450.
- Park, S.H.; Kim, Y.J.; Im, D.H.; Kim, C.K.; Jung, S.C.; Kim, H.J.; Jang, Y.; Kim, S.S. Development of Eco Driving System for Agricultural Tractor. *J. Biosyst. Eng.* **2010**, *35*, 77–84. [CrossRef]
- Jiang, J. Optimal Gain Scheduling Controller for a Diesel Engine. *IEEE Control Syst.* **1994**, *14*, 42–48. [CrossRef]
- Sung, S.W.; Lee, I.B. Limitations and countermeasures of PID controllers. *Ind. Eng. Chem. Res.* **1996**, *35*, 2596–2610. [CrossRef]
- Saunders, C.; Ucgul, M.; Godwin, R.J. Discrete element method (DEM) simulation to improve performance of a mouldboard skimmer. *Soil Tillage Res.* **2021**, *205*, 104764. [CrossRef]

20. Kim, W.S.; Kim, Y.J.; Baek, S.Y.; Baek, S.M.; Kim, Y.S.; Park, S.U. Development of a prediction model for tractor axle torque during tillage operation. *Appl. Sci.* **2020**, *10*, 4195. [[CrossRef](#)]
21. Kim, W.-S.; Kim, Y.-S.; Kim, Y.-J. Development of Prediction Model for Axle Torque of Agricultural Tractors. *Trans. ASABE* **2020**, *63*, 1773–1786. [[CrossRef](#)]
22. Kim, Y.S.; Kim, W.S.; Baek, S.Y.; Baek, S.M.; Kim, Y.J.; Lee, S.D.; Kim, Y.J. Analysis of tillage depth and gear selection for mechanical load and fuel efficiency of an agricultural tractor using an agricultural field measuring system. *Sensors* **2020**, *20*, 2450. [[CrossRef](#)]
23. Goering, C.E. *Engine and Tractor Power*; American Society of Agricultural Engineers (ASAE): St. Joseph, MI, USA, 1992.
24. Bietresato, M.; Friso, D.; Sartori, L. Assessment of the efficiency of tractor transmissions using acceleration tests. *Biosyst. Eng.* **2012**, *112*, 171–180. [[CrossRef](#)]
25. Chancellor, W.J.; Thai, N.C. Automatic Control of Tractor Transmission Ratio and Engine Speed. *Trans. ASAE* **1984**, *27*, 642–664. [[CrossRef](#)]
26. Zhang, N.; Perumpral, J.; Byler, R.K. Automatic control system for optimizing diesel engine performance. *Comput. Electron. Agric.* **1987**, *2*, 31–46. [[CrossRef](#)]
27. De Farias, M.S.; Schlosser, J.F.; Linares, P.; Bertollo, G.M.; Martini, A.T. Reduction of fuel consumption using driving strategy in agricultural tractor. *Rev. Bras. Eng. Agric. E Ambient.* **2019**, *23*, 144–149. [[CrossRef](#)]
28. Gui, X.Q.; Goering, C.E.; Buck, N.L. Simulation of a fuel-efficient augmented engine. *Trans. Am. Soc. Agric. Eng.* **1989**, *32*, 1875–1881. [[CrossRef](#)]
29. Li, B.; Sun, D.; Hu, M.; Liu, J. Research on economic comprehensive control strategies of tractor-planter combinations in planting, including gear-shift and cruise control. *Energies* **2018**, *11*, 686. [[CrossRef](#)]
30. Bera, P. Torque characteristic of SI engine in dynamic operating states. *Combust. Engines* **2017**, *171*, 175–180. [[CrossRef](#)]
31. Shafaei, S.M.; Kamgar, S. A comprehensive investigation on static and dynamic friction coefficients of wheat grain with the adoption of statistical analysis. *J. Adv. Res.* **2017**, *8*, 351–361. [[CrossRef](#)]
32. Kolator, B.; Białobrzewski, I. A simulation model of 2WD tractor performance. *Comput. Electron. Agric.* **2011**, *76*, 231–239. [[CrossRef](#)]
33. Knauder, C.; Allmaier, H.; Sander, D.E.; Sams, T. Investigations of the friction losses of different engine concepts. Part 1: A combined approach for applying subassembly-resolved friction loss analysis on a modern passenger-car diesel engine. *Lubricants* **2019**, *7*, 39. [[CrossRef](#)]
34. Renius, K.T. *Fundamentals of Tractor Design*, 1st ed.; Springer International Publishing: Cham, Switzerland, 2019; ISBN 978-3-030-32804-7.
35. Iqbal, M.Z.; Islam, M.N.; Chowdhury, M.; Islam, S.; Park, T.; Kim, Y.-J.; Chung, S.-O. Working Speed Analysis of the Gear-Driven Dribbling Mechanism of a 2.6 kW Walking-Type Automatic Pepper Transplanter. *Machines* **2021**, *9*, 6. [[CrossRef](#)]
36. Baek, S.M.; Kim, W.S.; Kim, Y.S.; Baek, S.Y.; Kim, Y.J. Development of a simulation model for HMT of a 50 kW class agricultural tractor. *Appl. Sci.* **2020**, *10*, 4064. [[CrossRef](#)]
37. Howard, C.N.; Kocher, M.F.; Hoy, R.M.; Blankenship, E.E. Testing the fuel efficiency of tractors with continuously variable and standard geared transmissions. *Trans. ASABE* **2013**, *56*, 869–879. [[CrossRef](#)]
38. Kim, Y.S.; Kim, W.S.; Siddique, M.A.A.; Baek, S.Y.; Baek, S.M.; Cheon, S.H.; Lee, S.D.; Lee, K.H.; Hong, D.H.; Park, S.U.; et al. Power transmission efficiency analysis of 42 kW power agricultural tractor according to tillage depth during moldboard plowing. *Agronomy* **2020**, *10*, 1263. [[CrossRef](#)]